Am J Transl Res 2026;18(5):4000-4009
www.ajtr.org /ISSN:1943-8141/AJTR0171037

Original Article

A preliminary study on quantitative assessment of apical lesion area

Huaxin Sui[1], Zheng He[1], Boyu Li[1], Yuchi Feng[1], Hu Chen[2,3,4,5]

[1]Department of Stomatology, Peking University First Hospital, Beijing 100034, China; [2]Center of Digital Dentistry, Peking University School and Hospital of Stomatology, Beijing 100081, China; [3]Department of Prosthodontics, Peking University School and Hospital of Stomatology, Beijing 100081, China; [4]National Engineering Laboratory for Digital and Material Technology of Stomatology, Beijing 100081, China; [5]NHC Key Laboratory of Digital Stomatology (Key Laboratory of Digital Stomatology, Chinese Academy of Medical Sciences), Beijing 100081, China

Received December 26, 2025; Accepted April 2, 2026; Epub May 15, 2026; Published May 30, 2026

Abstract: Objective: To establish a quantitative method for calculating the area of apical lesions, thereby enabling a more precise assessment of the extent of apical lesions. Methods: Three observers annotated periapical radiographs using a proprietary web-based annotation platform. Root outlines and lesion boundaries were delineated to obtain both the absolute lesion area (S_a) and the relative lesion area (S_r), calculated as the ratio of lesion area to root area. Observers also evaluated periapical status using the Periapical Index (PAI). All measurements were repeated after one month. Intra- and inter-observer reliability for PAI scores were assessed using Cohen's kappa and Fleiss' kappa, respectively, while reliability for S_a and S_r measurements was evaluated using the intraclass correlation coefficient (ICC). Agreement between repeated measurements was visualized using Bland-Altman plots. Results: Annotations were completed on 126 radiographs containing 490 tooth roots. PAI scores demonstrated moderate intra-observer (Cohen's kappa range: 0.45-0.58) and inter-observer (Fleiss' kappa: 0.41) reliability. In contrast, ICC values for both S_a and S_r indicated good to excellent reliability (range: 0.72-0.89). Intra-observer ICCs for S_r (range: 0.85-0.89) were consistently higher than those for S_a (range: 0.72-0.81). Bland-Altman analysis revealed that over 95% of the measurement differences fell within the limits of agreement for all observers. Conclusions: This study established a relatively quantitative method for assessing apical lesions. S_r demonstrated the highest consistency, followed by S_a, while PAI showed only moderate reliability. These findings support the potential of quantitative metrics as objective alternatives to traditional subjective scoring systems.

Keywords: Apical periodontitis, quantitative assessment, periapical index, intraclass correlation coefficient, bland-altman plot

Introduction

In oral clinical practice, apical periodontitis (AP) is a commonly encountered condition [1]. Histologically, it is primarily characterized by inflammatory cell infiltration and destruction of alveolar bone, while radiographically, it is manifested as radiolucent images in the periapical area. Comprehensive clinical evaluation and high-resolution imaging techniques are essential for AP diagnosis and the development of appropriate treatment strategies. Imaging examinations enable clear visualization of the periapical region and facilitate the identification of pathological changes at the root apex.

Cone beam computed tomography (CBCT) display three-dimensional visualization of AP lesions, while panoramic radiography enables a comprehensive observation of the overall oral cavity structure. Among these radiological examination methods, panoramic tomography has the lowest detection rate for apical lesions. As a result, it is mainly suitable for screening large-scale lesions [2]. In contrast, periapical radiography offers important evidence on the progression, regression, and persistence of AP [3]. It can also help determine the number of roots, their configuration, and the presence and location of apical lesions [4]. Leonardi Dutra et al. [5] found, through a meta-

https://doi.org/10.62347/ZSCV3463

analysis, that CBCT imaging provided excellent diagnostic accuracy for the detection of artificially created AP lesions [area under the curve (AUC) exceeding 80%], whereas periapical radiographs showed good accuracy (AUC ranging 70%-80%). While CBCT demonstrates greater sensitivity in detecting apical lesions [5, 6], it is associated with higher costs and greater radiation exposure (with operating parameters of 90 kV and 5.0 mA) than periapical radiography, violating the principle of *As Low As Reasonably Achievable* [7].

Furthermore, Araki et al. [8] reported certain limitations of CBCT imaging, among which relatively low contrast resolution may limit image clarity and diagnostic accuracy. In addition, adjacent high-density structures in CBCT images may lead to beam-hardening and scattering artifacts, further compromising image quality [9]. While CBCT offers advantages in three-dimensional imaging and lesion detection sensitivity, periapical radiography continues to play an irreplaceable role in routine clinical practice - particularly in initial diagnosis and treatment follow-up - due to the higher cost, radiation dose, and inherent technical limitations associated with CBCT [10].

In clinical practice, the evaluation of treatment outcomes for AP is often based on changes in the size of preapical lesions. A reduction in lesion size following root canal therapy indicates successful treatment, whereas unchanged or increased lesion size may suggest ineffective treatment. Once intelligent detection of periapical periodontitis has been achieved, further quantification of apical lesion size is necessary for a more precise assessment of disease status. The periapical index (PAI), a widely used scoring system, provides a structured framework for evaluating periapical status based on reference radiographs [11]. However, the PAI scoring process is relatively complex. It is labor-intensive and requires professional and systematic training to ensure the accuracy and reliability of scoring [12].

As a semi-quantitative tool, the PAI grading system is inherently subjective and may lack sufficient sensitivity to capture subtle changes in lesion size during treatment, underscoring the need for more precise quantitative assessment methods. Therefore, considering the widespread clinical use of periapical radiography and the limitations of existing semi-quantitative evaluation methods (such as the PAI), this study aims to establish a quantitative method based on periapical radiographs to calculate the area of periapical lesions, thereby enabling a more accurate and objective assessment of lesion extent and its dynamic changes.

Materials and methods

Sample collection

Periapical radiographs collected in the Department of Stomatology at Peking University First Hospital over the past five years were used in this retrospective study. Radiographic images of dental periapical area were acquired using fluorescent plate system (VistaScan, Dürr Dental, Bietigheim-Bissingen, Germany). The images were scanned and processed using the VistaScan Mini scanner (Dürr Dental, Bietigheim-Bissingen, Germany). All periapical radiographs were acquired using parallel technique to minimize image distortion and magnification differences. The exposure parameters were set as follows: tube voltage 65 kVp, tube current 7 mA, and exposure time 0.125-0.250 seconds. The scanned images were stored in a computer database, allowing for efficient storage and retrieval of radiographic data. The study was approved by the Ethics Committee of Peking University First Hospital (2025R0582-0002).

Inclusion criteria: (1) Teeth corresponding to the selected radiographs had been clinically diagnosed with AP; (2) Radiographs with appropriate exposure parameters and image quality, ensuring that lesions could be clearly identified; and (3) Periapical radiographs of permanent teeth. Exclusion criteria: (1) Lesions involving adjacent anatomical structures with extensive cortical bone destruction; (2) Severe periodontal disease; (3) Severe distortion of teeth in the image; (4) Images that are too bright or dark, preventing clear identification of lesions; (5) Presence of deciduous teeth in the radiographs.

Annotation of the digital dental periapical radiographs

Digital dental periapical radiographs were systematically annotated using a proprietary web-

Table 1. The criteria for PAI scoring

PAI scores	Criteria
1	Normal periapical structures
2	Small changes in bone structure
3	Changes in bone structure with some mineral loss
4	Periodontitis with well-defined radiolucent areas
5	Severe periodontitis with exacerbating features

Abbreviations: PAI: periapical index.

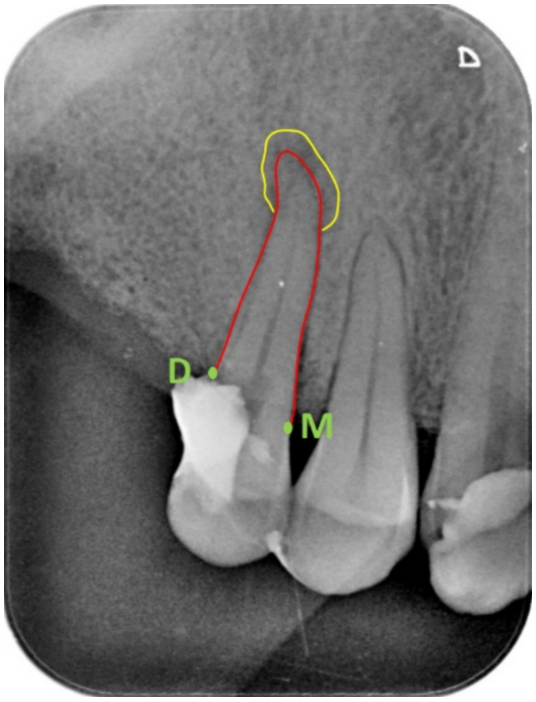

Figure 1. Representative periapical radiograph illustrating the annotation method. Point M - mesial cementoenamel junction, Point D - gingival margin of distal tooth defect, Red Curve - external boundary of the root between Point D and M; Yellow Curve - the maximum extent of the periapical radiolucent area identified by the observer.

based annotation platform developed at our institution. This platform incorporated customized tools for standardized radiographic assessment and data collection. After being informed of the study objectives and the diagnostic tasks, three observers (Dr. HZ, LBY, and SHX; clinical experience of 3-10 years) independently performed the annotation of the periapical area using the polygonal annotation tool.

For the assessment of the PAI, a preliminary phase was conducted prior to formal evaluation of the radiographs. During this phase, the observers were presented with reference radiographs and detailed guidelines for each scoring category according to the criteria outlined by Orstavik et al. (**Table 1**) [13]. To ensure consistency in defining lesion boundaries, particularly in ambiguous cases where widening of the periodontal ligament space may be difficult to distinguish from an early lesion, the observers jointly participated in a calibration exercise. This exercise was conducted independently of the formal study dataset. A training set consisting of 20 periapical films, encompassing a spectrum from healthy teeth to those with clear periapical radiolucencies, was selected. The observers first completed the annotation and scoring independently. Subsequently, a consensus meeting moderated by the researcher was conducted to compare the delineated lesion boundaries and discuss discrepancies. For cases with significant disagreement, a consensus interpretation of the PAI scoring criteria and the definition of the "periapical lesion boundary" was established through discussion. For example, the disruption of the continuity of the periodontal ligament space was defined as a key criterion for early identification of lesion. This calibration process was designed to minimize systematic bias among observers and to standardize the interpretation of lesion boundaries. The results of this calibration exercise were not included in the final statistical analysis.

Subsequently, the observers annotated the outlines of the root (red curve) and the boundary of the apical lesions (yellow curve). The area enclosed between the red and yellow curves represented the absolute area of apical lesions (S_a). To reduce the influence of radiographic projection angle and magnification differences, the relative area of apical lesions (S_r) was calculated as the ratio of the lesion area to root area (**Figure 1**). During the annotation process, observers used image magnification and contrast enhancement tools to capture details. Color coding was applied to clearly distinguish different situations, with different colors corresponding to different tooth roots and types of root tip lesions. After completing the annotation, observers recorded the anatomical location of the tooth and assigned the corresponding PAI score.

All annotations were performed on digital monitors (Dell Inc., Texas, USA). During the labeling process, the observers were blinded to the clinical diagnosis and were required to annotate and score all intact teeth present in the radiographs. To evaluate intra-observer and inter-observer reliability, the observers repeated the annotation and scoring procedures after a predefined interval. All observers worked independently without mutual influence, and during the second assessment, they were prohibited from referencing their initial evaluations. Additionally, they were not permitted to exchange opinions regarding the evaluation criteria or specific cases.

Statistical analysis

SPSS statistical software was used for statistical analysis. To assess inter-observer reliability of the PAI scores, the overall agreement among observers was evaluated using Fleiss' kappa coefficient, whereas intra-observer reliability was assessed using Cohen's kappa coefficient by comparing the two scoring sessions for each observer. The scoring criteria were 0.81-1 (almost perfect agreement), 0.61-0.80 (substantial agreement), 0.41-0.60 (moderate agreement), 0.21-0.40 (fair agreement), and 0-0.20 (slight agreement), respectively.

For the quantitative measurements of S_a and S_r, inter-observer reliability was assessed using the intraclass correlation coefficient (ICC) based on a two-way random-effects model with an absolute agreement definition and single-measurement type. Intra-observer reliability was also evaluated using the ICC, calculated based on a two-way mixed-effects model with an absolute agreement definition and single-measurement type, to determine the consistency between the two measurements obtained by each observer. The scoring criteria for ICC were 0.9-1 (excellent reliability), 0.75-0.89 (good reliability), 0.5-0.74 (moderate reliability), and 0-0.5 (poor reliability), respectively.

The level of agreement between repeated measurements for each observer was visually assessed using Bland-Altman plots, which display the mean difference and the 95% limits of agreement (LoA). The distribution pattern of data points was examined to identify potential systematic bias or proportional bias. A P value < 0.05 was considered statistically significant.

Sample size consideration

Due to the retrospective nature of this study, a formal a priori sample size calculation was not performed. We included all eligible periapical radiographs obtained at our department during the five-year period. To assess whether the sample size was sufficient for reliability analysis, a post-hoc precision analysis was conducted. Specifically, the width of the 95% confidence intervals (CIs) for the primary outcome measures (Kappa and ICC) was examined. Narrow CIs indicate high precision of the estimated agreement. As shown in the results, the CIs for both Kappa and ICC values were relatively narrow (e.g., overall Fleiss' Kappa 95% CI width: 0.065; overall ICC 95% CI width: 0.040), suggesting that the sample size of 126 radiographs (490 roots) was adequate to provide stable and precise estimates of observer agreement.

Results

A total of 126 digital periapical radiographs were collected, including maxillary incisors, mandibular incisors, maxillary canines, mandibular canines, maxillary premolars, mandibular premolars, maxillary molars, and mandibular molars, with corresponding counts of 19, 12, 13, 16, 64, 71, 37, and 100, respectively.

Representative examples of the radiographic annotation process are shown in **Figure 2**. Different colored curves represent the boundaries of the apical lesions and the root contours, while labels of the same color correspond to the corresponding tooth position and PAI score. During the annotation process, the platform automatically generated a result table containing the serial number, image identifier, annotation coordinates, and corresponding labels (**Table 2**). Examples of annotation for different tooth positions are shown in **Figure 3**.

The Cohen's kappa and Fleiss' kappa values are listed in **Table 3**. The kappa values for the three observers were in the moderate agreement range (0.41-0.60). The ICC values are shown in **Table 4**. ICC values for the quantitative measurements demonstrated good agreement (0.75-0.89) among observers. In addition, the inter-observer ICC values for S_r were higher than those for S_a, indicating better reproducibility for the relative lesion area measurement.

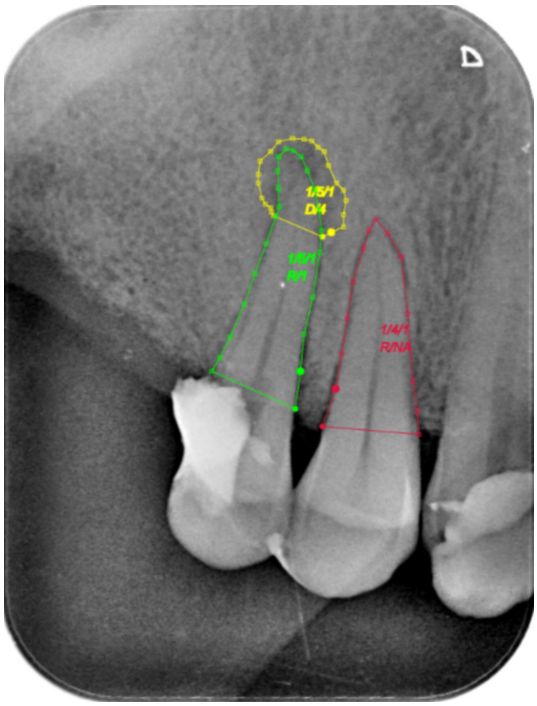

Figure 2. Example of annotation on periapical radiographs. (THE green curve outlines the root of the right maxillary second premolar, and the yellow curve delineates the corresponding apical lesion; The red outlines the root of the right maxillary first premolar. No apical lesion boundary was annotated for the right maxillary first premolar because the observer did not identify any periapical radiolucency around its root).

The mean difference between the two measurements obtained by each observer are shown in **Table 5**. The Bland-Altman plots demonstrated that most points fell within the 95% LoA (**Figure 4**). However, the distribution of points exhibited a funnel-shaped pattern rather than a random scatter.

Discussion

The interpretation of radiographic images, including CBCT, may be partly subjective, highlighting the need for standardized assessment tools and calibration between examiners [14]. As a recognized scoring system, the reliability of PAI remains at a relatively low level. In the present study, the quantitative assessment method established for measuring apical lesion area was compared with the PAI system to preliminarily evaluate its reliability.

In this study, the three observers were unaware of the tooth positions affected by AP before annotation, and they made subjective judgments on the location of apical lesions, which made the results more authentic and reliable. In this study, several methodological measures were implemented to minimize potential sources of variability. First, the observation environment was standardized across the two evaluation sessions. All observers performed the assessments in the same room, using the same computer monitor to view images, and the lighting conditions were kept consistent. Second, to minimize potential recall bias, a one-month interval was set between the two evaluation sessions for each observer when re-assessing the same digital radiographs.

Based on the intra- observer reliability results of the three observers, the consistency of PAI scores was the lowest, which is consistent with previous findings [12]. One potential explanation is that PAI is inherently subjective and relies heavily on the observer's clinical experience; therefore, it may not fully reflect the actual severity of periapical lesions. In contrast, both S_r and S_a provide quantitative measurements of apical lesions, enabling a more objective assessment of the extent of apical lesions. However, regarding inter-observer reliability, the PAI scores in this study showed only moderate agreement (kappa values), which differs from the findings reported by Tarcin et al. [12]. In that study, a higher inter-observer agreement was reported, with a mean kappa value of 0.39 for PAI and 87.0% agreement after dichotomization. Several factors may account for this discrepancy. First, while the one-month interval between the two annotation sessions may have contributed to memory bias, differences in observer training may play a crucial role. In the study by Tarcin et al., the observers may have undergone more standardized and systematic training with reference radiographs, which could have facilitated a more consistent interpretation of the PAI scoring categories [12]. Second, differences in the composition of observer experience may also have influenced the results. In the present study, the observers had 3-10 years of clinical experience, whereas the professional backgrounds of the observers in the study by Tarcin et al. were unclear [12]. Variability in observer experience may therefore have influenced the agreement level. Furthermore, differences in study subject characteristics, including lesion complexity, image quality, and sample sizes,

Table 2. Result list

Serial Number	Picture Number	X	Y	Labels
16426	3007472	372,388,398,393,386	275,258,238,224,201	1/5/1/D/4
16427	3007472	342,348,352,362,370	476,433,391,349,298	1/5/1/R/1
16605	3007472	373,388,395,401,408	496,453,413,373,331	1/4/1/R/NA

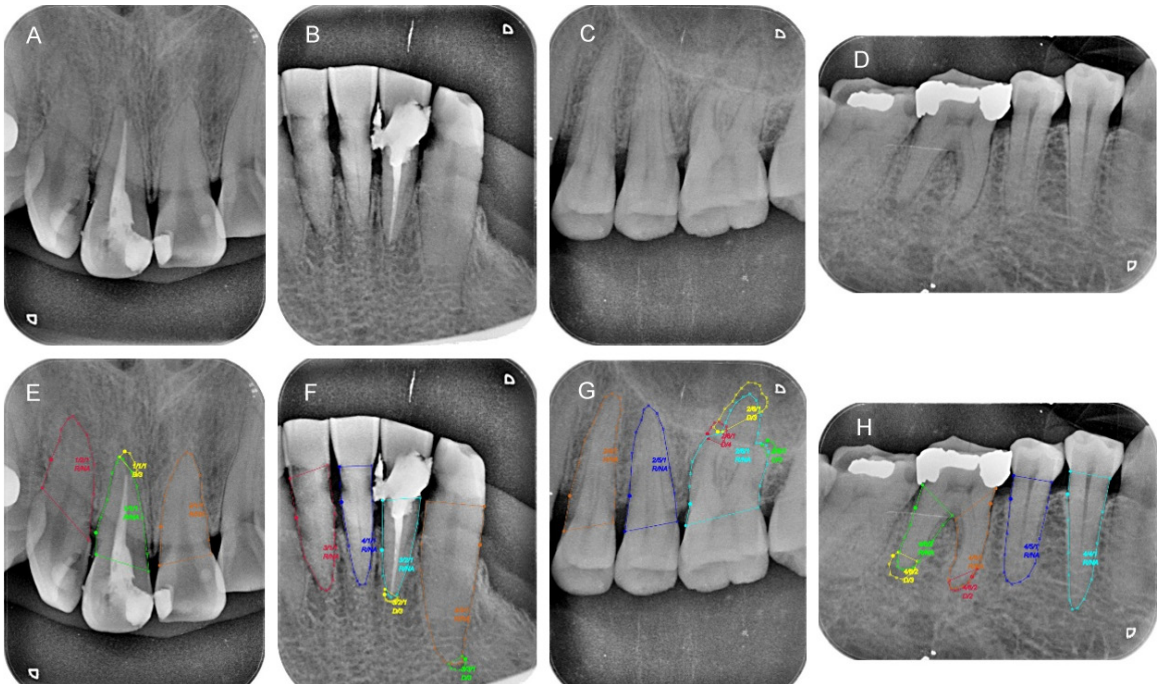

Figure 3. Annotation examples for different tooth positions. A, E: Pre - and Post - annotation images of maxillary anterior teeth; B, F: Pre- and post-annotation images of mandibular anterior teeth; C, G: Pre- and post-annotation images of maxillary premolars and molars; D, H: Pre- and post-annotation images of mandibular premolars and molars.

Table 3. Cohen's kappa and Fleiss' kappa values

	Cohen's Kappa (95% CI)			Fleiss' Kappa (95% CI)
	SHX	HZ	LBY	
PAI scores	0.572 (0.518-0.627)	0.584 (0.530-0.639)	0.449 (0.384-0.514)	0.532 (0.499-0.564)

Abbreviations: PAI: periapical index; CI: confidence interval. SHX, HZ, and LBY are the names of the three observers, who are physicians with 3 to 10 years of clinical experience.

Table 4. ICC values

	Intra-observer's ICC (95% CI)			Inter-observer's ICC (95% CI)
	SHX	HZ	LBY	
S_a	0.831 (0.798-0.859)	0.871 (0.845-0.893)	0.810 (0.774-0.841)	0.872 (0.851-0.891)
S_r	0.851 (0.822-0.876)	0.840 (0.809-0.867)	0.835 (0.803-0.862)	0.896 (0.878-0.911)

Abbreviations: ICC: correlation coefficient; CI: confidence interval; S_a: absolute area of apical lesions; S_r: relative area of apical lesions. SHX, HZ, and LBY are the names of the three observers, who are physicians with 3 to 10 years of clinical experience.

may also have impacted the results. It is noteworthy that Tarcin et al. also reported that dichotomization of the PAI scores significantly improved observer agreement, suggesting that when the PAI is used as a five-point scale, the differentiation between intermediate cate-

Table 5. Average difference between S_a and S_r marked by each observer

	Average Difference (95% CI)		
	SHX	HZ	LBY
S_a	119.188 (-1725.910; 1964.287)	-224.239 (-2475.610; 2027.130)	-349.896 (-3104.710; 2404.918)
S_r	0.010 (-0.112; 0.131)	-0.018 (-0.093; 0.135)	-0.027 (-0.174; 0.119)

Abbreviations: CI: confidence interval; S_a: absolute area of apical lesions; S_r: relative area of apical lesions. SHX, HZ, and LBY are the names of the three observers, who are physicians with 3 to 10 years of clinical experience.

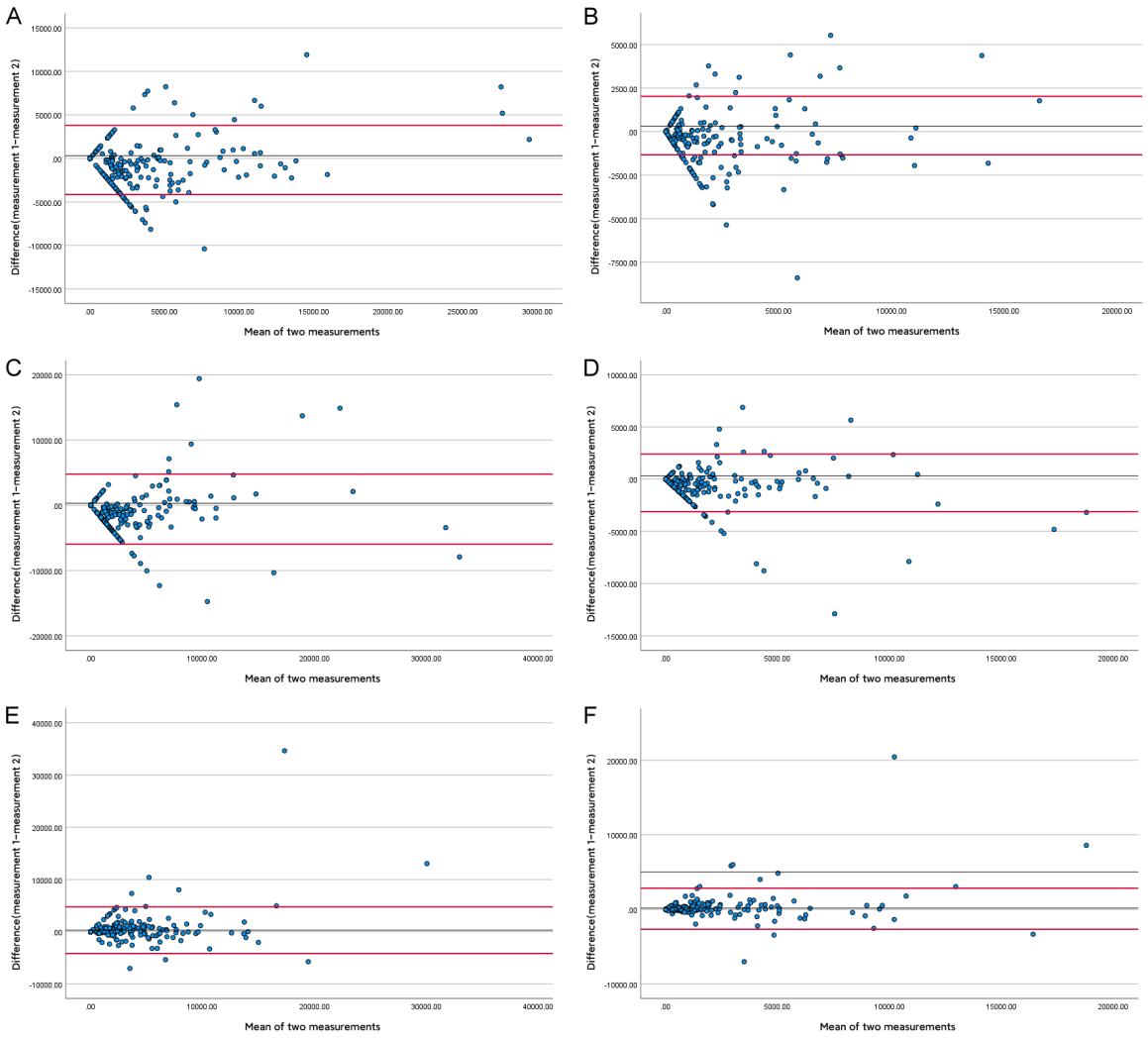

Figure 4. Bland-Altman plots illustrating the agreement between repeated measurements. A: Agreement of S_a between the two measurements performed by HZ, with 15 points outside the LoA; B: Agreement of S_r between the two measurements performed by HZ, with 12 points outside the LoA; C: Agreement of S_a between the two measurements performed by LBY, with 43 points outside the LoA; D: Agreement of S_r between the two measurements performed by LBY, with 31 points outside the LoA; E: Agreement of S_a between the two measurements performed by SHE, with 14 points outside the LoA; F: Agreement of S_r between the two measurements performed by SHE, with 16 points outside the LoA. The black lines represent the mean difference, and the red lines indicate the 95% LoA. Abbreviations: LoA: limits of agreement; S_a: absolute area of apical lesions; S_r: relative area of apical lesions.

gories (e.g., scores 2, 3, and 4) represents a major source of inter-observer variability [12]. The findings of this study further confirm the limitations of PAI in fine grading and highlight the necessity of developing more objective quantitative indicators (such as S_r and S_a).

Regarding the quantitative measurements, S_r demonstrated the highest inter-observer reliability, followed by S_a. One possible explanation is that S_r represents the ratio of S_a to the root area, partially compensating variations in the projection angle and magnification of periapical radiographs. Given that variations in radiographic projection angles may occur when imaging the same tooth at different time points, simply comparing the apical lesion area (i.e., S_a) may introduce measurement errors.

Bland-Altman plots are a widely used statistical method for evaluating the agreement between two measurement methods or the repeatability of a single method [15, 16]. This method visualizes the differences between two measurements against their mean values, providing insights into systematic bias, proportional bias, and LoA [15]. An essential aspect of Bland-Altman analysis is the visual inspection of the distribution pattern of data points. A random distribution of points around the mean difference line, with most points falling within the LoA, indicates good agreement [16, 17]. In this study, most data points were located within the LoA. However, the distribution of points exhibited a funnel-shaped pattern rather than a random scatter, suggesting that the measurement variability increased as the means value increased. This indicates that larger apical lesions may be associated with greater variability in lesion boundary identification.

Periapical radiographs have inherent limitations. As two-dimensional images, they can only depict the mesiodistal and apicocoronal extent of lesions. In comparison, three-dimensional CBCT has significant advantages. It not only enables two-dimensional visualization of lesions but also allows the evaluation of lesion depth [2, 18]. During two-dimensional evaluation, the lack of depth information can easily lead to evaluation bias. Previous studies have demonstrated that when mineral loss of the cortical bone plate does not reach a certain level, lesions may be difficult to detect on periapical radiographs [19]. In addition, CBCT can eliminate the covering of the cheekbone plate, allowing the cortical plate to be clearly exposed and accurately delineating the boundaries of lesions. Another limitation of periapical radiographs is the overlapping of root structures, which may affect observation and diagnostic judgment. Gudac et al. [14] found that CBCT can identify a greater number of root canals compared with periapical radiography, particularly in premolars and molars. Although these features make CBCT an appealing alternative to traditional periapical radiographs, its higher sensitivity also means that very small areas of unmineralized tissues in the apical region may be detected. Even when these tissues are undergoing healing, they may be misinterpreted as signs of treatment failure [20]. Consequently, periapical radiography continues to play an irreplaceable role in the follow-up evaluation after root canal treatment. This study has established a relatively quantitative method for detecting apical lesions, which facilitates a more intuitive and accurate comparison of the changes in the extent of apical lesions during follow-up and allows for the calculation of the healing rate of apical lesions at different stages, thereby holding great clinical significance.

This study has several limitations. First, it was a single-center retrospective study with a relatively limited sample size, which may affect the generalizability of the findings. Second, the evaluation was based on two-dimensional periapical radiographs, which cannot fully reflect the three-dimensional volume of apical lesions. Future research could incorporate CBCT for validation through three-dimensional volumetric measurements.

Conclusion

This study successfully established and preliminarily validated a periapical radiograph-based method for quantitative assessment of apical lesion area. S_r demonstrated the highest consistency, in terms of both intra- and inter-observer reliability, outperforming S_a and the traditional PAI scoring system. This method provides a new tool for the objective and quantitative monitoring of changes in apical lesions during clinical follow-up.

Acknowledgements

This study was funded by the National High Level Hospital Clinical Research Funding (Scientific Research Seed Fund of Peking University First Hospital) (No. 2024SF32), Beijing Natural Science Foundation (L242114) and the Non-profit Central Research Institute Fund of Chi-

nese Academy of Medical Sciences (2023-PT320-09).

Disclosure of conflict of interest

None.

Address correspondence to: Dr. Hu Chen, Center of Digital Dentistry, Peking University School and Hospital of Stomatology, No. 22, Zhongguancun South Street, Haidian District, Beijing 100081, China. Tel: +86-17813005960; Fax: +86-010-62142111; E-mail: ccenhu@126.com

References

[1] Wen YH, Lin YX, Zhou L, Lin C and Zhang L. The immune landscape in apical periodontitis: from mechanism to therapy. Int Endod J 2024; 57: 1526-1545.

[2] Elheeny AAH and Tony GE. Two-dimensional radiographs and cone-beam computed tomography assessment of concentrated growth factor and platelet-rich fibrin scaffolds in regenerative endodontic treatment of immature incisors with periapical radiolucency: a randomized clinical trial. J Endod 2024; 50: 792-806.

[3] Stera G, Giusti M, Magnini A, Calistri L, Izzetti R and Nardi C. Diagnostic accuracy of periapical radiography and panoramic radiography in the detection of apical periodontitis: a systematic review and meta-analysis. Radiol Med 2024; 129: 1682-1695.

[4] Gurusamy K, Duhan J, Tewari S, Sangwan P, Gupta A, Mittal S, Kumar V and Arora M. Patient-centric outcome assessment of endodontic microsurgery using periapical radiography versus cone beam computed tomography: A randomized clinical trial. Int Endod J 2023; 56: 3-16.

[5] Leonardi Dutra K, Haas L, Porporatti AL, Flores-Mir C, Nascimento Santos J, Mezzomo LA, Corrêa M and De Luca Canto G. Diagnostic accuracy of cone-beam computed tomography and conventional radiography on apical periodontitis: a systematic review and meta-analysis. J Endod 2016; 42: 356-364.

[6] Saidi A, Naaman A and Zogheib C. Accuracy of cone-beam computed tomography and periapical radiography in endodontically treated teeth evaluation: a five-year retrospective study. J Int Oral Health 2015; 7: 15-19.

[7] Special Committee to Revise the Joint AAE/AAOMR Position Statement on use of CBCT in Endodontics. AAE and AAOMR joint position statement: use of cone beam computed tomography in endodontics 2015 update. Oral Surg Oral Med Oral Pathol Oral Radiol 2015; 120: 508-512.

[8] Araki K, Maki K, Seki K, Sakamaki K, Harata Y, Sakaino R, Okano T and Seo K. Characteristics of a newly developed dentomaxillofacial X-ray cone beam CT scanner (CB MercuRay): system configuration and physical properties. Dentomaxillofac Radiol 2004; 33: 51-59.

[9] Templier L, Rossi C, Lagravère Vich M, Fernández Pujol R, Muwanguzi M and Gianoni-Capenakas S. Are multi-detector computed tomography and cone-beam computed tomography exams and software accurate to measure the upper airway? A systematic review. Eur J Orthod 2023; 45: 818-831.

[10] Chaudhary S, Singh H, Gharti A, Chaudhary GK and Gupta A. Radiographic evaluation of preoperative periapical status in teeth with apical abscess. Journal of Kathmandu Medical College 2023; 12: 87-95.

[11] Yildiz B, Dumani A, Isci AS, Sisli SN, Tumani Ustdal B and Yoldas O. Outcome of single-visit root canal treatment with or without MTAD: a randomized controlled clinical trial. Int Endod J 2024; 57: 2-11.

[12] Tarcin B, Gumru B, Iriboz E, Turkaydin DE and Ovecoglu HS. Radiologic assessment of periapical health: comparison of 3 different index systems. J Endod 2015; 41: 1834-1838.

[13] Orstavik D, Kerekes K and Eriksen HM. The periapical index: a scoring system for radiographic assessment of apical periodontitis. Endod Dent Traumatol 1986; 2: 20-34.

[14] Gudac J, Hellén-Halme K, Venskutonis T, Puisys A and Machiulskiene V. Comparison of selected anatomical and treatment-related diagnostic parameters estimated by cone-beam computed tomography and digital periapical radiography in teeth with apical periodontitis. J Oral Maxillofac Res 2020; 11: e4.

[15] Ekstrøm CT and Carstensen B. Statistical models for assessing agreement for quantitative data with heterogeneous random raters and replicate measurements. Int J Biostat 2024; 20: 455-466.

[16] Cesana BM and Antonelli P. Bland and Altman agreement method: to plot differences against means or differences against standard? An endless tale? Clin Chem Lab Med 2024; 62: 262-269.

[17] Moore AR. A review of Bland-Altman difference plot analysis in the veterinary clinical pathology laboratory. Vet Clin Pathol 2024; 53: 75-85.

[18] Mosquera-Barreiro C, Ruíz-Piñón M, Sans FA, Nagendrababu V, Vinothkumar TS, Martín-González J, Martín-Biedma B and Castelo-Baz P. Predictors of periapical bone healing associated with teeth having large periapical lesions following nonsurgical root canal treat-

ment or retreatment: a cone beam computed tomography-based retrospective study. Int Endod J 2024; 57: 23-36.

[19] Kim JH, Lee W, Kim KS, Roh YC, Kim DS and Lee BD. Quantitative analysis of periapical lesions on cone beam computed tomograph and periapical radiograph. Imaging Science in Dentistry 2009; 39: 41-49.

[20] Parmar PD, Dhamija R, Tewari S, Sangwan P, Gupta A, Duhan J and Mittal S. 2D and 3D radiographic outcome assessment of the effect of guided tissue regeneration using resorbable collagen membrane in the healing of through-and-through periapical lesions - a randomized controlled trial. Int Endod J 2019; 52: 935-948.